

The Microstructural Evaluation and Mechanical Properties of Al 6061-T6 Friction Stir Welding Joint with Varied Parameters

Mohamed Ackiel Mohamed^{1,a}, Yupiter HP Manurung^{2,b}, Mohd Kamil Md Said^{1,c},
Khairudin Salim^{1,d}, Siti Wan Zuraine^{1,e}

¹University Kuala Lumpur Malaysia France Institute, Bandar Baru Bangi, Selangor, Malaysia.

²Universiti Teknologi MARA (UiTM), 40450, Shah Alam, Selangor, Malaysia.

Abstract

Friction stir welding is an effective process for joining aluminium alloys and can significantly diminishes grain measure giving superb plastic deformation properties. Therefore, Friction stir welding is utilized in a wide range of welding applications that requires lightweight designs and increased joint reliability. The present experimental work examines the microstructural development and mechanical properties of friction stir welded Al 6061-T6 with varied welding parameters. The joining process was conducted with varied process parameters namely the rotational speed and traverse speed on butt joints with plate thickness of 6mm. The experimental method was based on a full factorial design with varied parameters between 350-1400 rpm and 0.2-4.6 mm/s for rotational speed and traverse speed respectively utilizing three levels for each parameter. The effect of zone formation on tensile strength properties and hardness profile were discussed and concluded. The best mechanical properties are obtained at higher traverse speeds with moderate rotational speed probably owing to the incidence of homogeneous grains and higher heat input. Two parameter variations displayed a combination of good weld class quality and mechanical properties namely rotation speed 950rpm with 4.6 mm/s traverse speed as well as 650 rpm rotation speed with 2.4 mm/s traverse speed.

Keywords: Friction stir welding; AA6061; full factorial design; microstructure; mechanical properties

INTRODUCTION

The broad use of aluminum alloys in an extensive variety of applications and the problems confronted in joining the alloys utilizing the typically used fusion welding methods have made friction stir welding (FSW) a predominant choice over the previous. Invented in the welding Institute (TWI) UK in 1991, FSW is an ecological amicable energy saving solid state joining process without the use of consumables. A pivoting shaft is embedded and moved along the adjoining surfaces of two inflexibly fastened plates put on a support plate. The

Resulting downward force and the frictional heating caused by the rotation of the shaft causes the material to diminish offering route to the approaching shaft, known as the tool pin. The pin is then moved in the transverse direction, causing the softened material to be dislocated from the frontal to the rear of the tool while undergoing whirling and stirring thus forming a solid joint. The fast adaption of FSW since its origin to the scholarly and modern world is closely related to the many points of interest credited to FSW contrasted with the normally utilized fusion welding because of its tendency of not achieving the melting temperature.

Among the most critical favourable circumstances which are conceivable to be accomplished by utilizing FSW are the better microstructure in the stir zone, extremely negligible distortion and shrinkage from solidification, insignificant stress concentration and weld imperfections. There are some principle parameters to be controlled amid welding to be specific the rotation speed, travel speed and downward force of the tool. However the pin geometry and depth, , tilt angle, crevices, finishing, backing material and cooling conditions, can add to the FSW influencing parameters[1, 2]. A typical example of a FSW butt weld joint is shown in Fig 1.

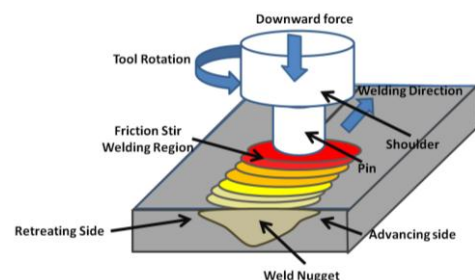


Figure 1: The friction stir welding process

Industrial applications which required designs with sufficient strength and lightweight materials faced undesirable circumstances when applying the frequently used fusion

welding joining process into these joints. Hence the invention of friction stir welding (FSW) created a huge interest from these numerous applications in varied industries, as it was proven to be far more favourable than joint produced using fusion welding. The superiority of FSW compared to fusion welding process such as gas metal arc welding (GMAW) and gas tungsten arc welding (GTAW) was perceived by A. K. Lakshminarayanan et al. [3] in their attempt of comparing the joint mechanical properties such as the micro hardness, fracture surface morphology, tensile properties, and the microstructure profiles. The dominance of FSW over the fusion welding process in the obtained mechanical properties mentioned was mainly attributed to the equivalently dispersed precipitates and fine grains in the stir zone overserved in FSW.

The existence of the oxide layer in some aluminium alloys requires broad surface preparation prior to being welded using the resistance welding process. However, FSW can be utilized to join most Aluminum combinations as the surface oxide is not an obstacle for the procedure and in this way no specific cleaning operation is required preceding welding. Substantially higher mechanical properties can be achieved using FSW as the joint does not experience the molten state (particularly when consideration is centered around heat-treatable light alloys) as contrasted with those given by customary procedures. Detrimental mechanical properties caused by the cycle of melting and re-solidification in fusion welding process is absent in FSW prompting enhanced mechanical properties, for example, strength, ductility and quality in some alloys [2-5]. Along these lines, the welds are portrayed by low distortion, decrease the residual stress and nonappearance of small scale deformities and subsequently the items dimensional dependability. The present work is aimed at the evaluation of mechanical and microstructural behavior of Al 6061-T6 plates obtained by employing different FSW parameters.

EXPERIMENTAL PROCEDURE

This study utilized 6mm thick Al6061 plates with T6 heat treatment designation. Two aluminium plates of 250mm ×100mm without any edge preparation and arranged in a butt joint type manner was placed above an even copper backing plate. Before setting the plates, the edges of the plates were appropriately cleaned by utilizing acetone. The abutting plates were solidly clamped to abstain from slipping and partition amid welding from the adjoining joint line.

The welding was executed using constant axial loading, 8KN with variable rotational and traverse speeds. In view of the thickness of the plate, the length of the pin was properly chosen. The proportion of distances across of the shoulder and pin was kept up consistent with a specific end goal to make the required weight for reconsolidation of material as well as to maintain a strategic distance from the escape of material amid

welding. The friction stir welding procedure and device profile utilized is delineated in Fig. 2.

The FSW was conducted with a tool containing a cylinder-shaped pin with a diameter of 6mm, a shoulder with 18mm diameter and a shoulder length measuring 24mm. The pin at the edge of the tool measured 5.5mm in total length, 0.5mm shorter than the material thickness of 6mm. The holder that was inserted in the clamp had a diameter of 10mm and measured 20mm in length. The routinely used material for machining tools, namely the H-13 with an air hardening 5% chromium tool steel was used to fabricate the FSW tool. This type of material is known as a prevalent choice for various cold work and hot work applications.

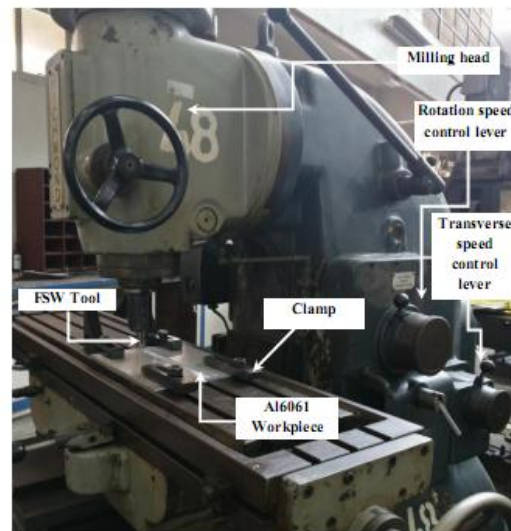


Figure 2: Friction stir welding process using a conventional milling machine

The microstructural assessment in FSW joints were observed visibly at various parameter variations. Specimens were taken from each welded plate for tensile, hardness tests and maro profile. Before hardness tests were performed, tests were set up by the typical metallurgical cleaning techniques and etched with Keller's reagent and the resulting weld zone was observed utilizing a metallurgical magnifying lens interfaced with a image examination framework. Three tensile specimens were taken from the same welded plate for every parameter combination executed. Tensile tests were performed under a cross head speed of 5 mm/min as indicated by the EN-895-2002 standard. The room temperature elasticity of the base and the friction stir welded sheet was assessed by performing tensile tests on a 250KN Instron universal testing machine. A high resolution extensometer was utilized amid uniaxial tensile tests. The hardness field was built up in the mid thickness (center level) of the cross area of the weld crease as indicated by the ISO 6507-2 standard with 3 measured points in the stir zone utilizing a Struers Duramin Micro-Vickers Hardness test machine with a 1kgf load.

RESULTS AND DISCUSSION

A. Macrostructure and Microstructure

Fig. 3 and 4 shows the obtained macrostructures of the weld joint cross sectional area for the different parameter variations of various rotation and traverse speeds utilized in FSW of AA 6061. The resulting macrostructures in the nugget zone (NZ) for a large portion of the parameter blend frames a basin and bowl like symmetrical shape. The shape of the cylindrical tool and probe used in the study essentially caused the above mentioned shapes. Be that as it may, at higher rotation speeds to be specific 1400 rpm, contorted awry shapes are framed. These formations are nearly ascribed to the uneven circulation of the material amid the mixing and spinning process during the FSW process due to larger heat input brought about by the utilization of greater rotation speed consolidated with lower traverse speed. It can be perceived that the widths of all the bowl and basin shaped NZ contrasts as needs be to the diverse parameter varieties utilized.

The width of NZ, TMAZ and the HAZ are significantly impacted by the tool rotation speed and the traverse speed. An expansion in the rotation speed causes a more extensive NZ and HAZ in the FSW joint while a diminishing traverse speed delineates a decrease in the NZ width. High and expanded tool rotation speed joined with a consistent traverse speed brought about serious plastic flow because of the huge measure of resulting heat input created. On the other hand utilizing a steady rotation speed with high traverse speed produces small heat input and less plastic flow. In spite of the fact that the rotation and traverse speed are both controlling parameters of an ordinary FSW joint, the tool rotation speed has more prominent impact on the result of the NZ, TMAZ and HAZ width contrasted with the traverse speed.

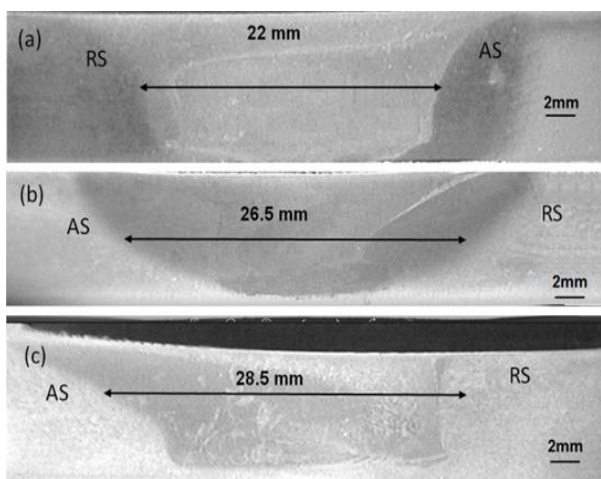


Figure 3: Transverse section macrographs for the joints obtained at the welding speed of 0.8 mm/s: (a) 650 rpm, (b) 950 rpm, and (c) 1400 rpm

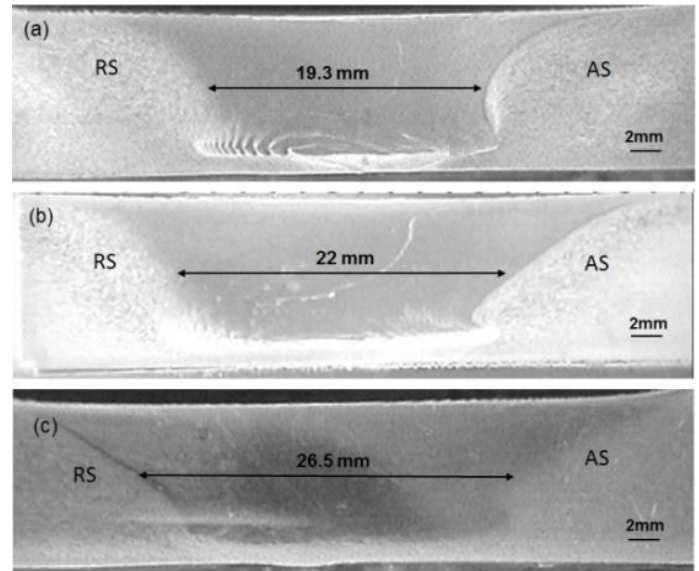


Figure 4: Traverse section macrographs for the joints obtained at the welding speed of 1.42 mm/s: (a) 650 rpm, (b) 950 rpm, and (c) 1400 rpm

The acquired macrographs in Fig. 4 demonstrates a more articulated appearance of the TMAZ in the AS with an estimated width of 230 μm while the RS demonstrates no strong sign of TMAZ development. The parameter blend of 950 rpm and 0.8 mm/s experienced the occurrence of TMAZ on both the RS and in addition the AS with a most extreme width magnitude of 320 μm . The material deformation on AS are more extreme than on RS. A noticeable amount of TMAZ development was seen in the AS for the joint made using 1400 rpm and 1.42 mm/s with very much less material deformation on the RS having similar appearance to the joint with a parameter variation of 0.8 mm/s and 650 rpm.

In contrast with the RS, all the parameter combination created a bigger width of TMAZ on the AS side. For the traverse speed of 0.8 mm/min, the TMAZ of the weld acquired utilizing high revolution speed is more extensive than that of the weld acquired utilizing low traverse speed either on AS or RS. It was noted that when the rotation speed of 1400 rpm was used, a reduced size was observed in the width on both AS and RS when utilizing high traverse speed compared to utilizing low traverse speed. Therefore, it can be said that the width of the TMAZ is indeed influenced by both the rotation speed and also the traverse speed. This is actuated by different energy input following from a variety of welding parameters blends. The material flow in the NZ boundary because of the vast energy input makes the material at TMAZ effectively distort and turn out to be soft. This plainly indicates the energy input escalates with the expanding of the tool rotation speed and the diminishing of traverse speed.

The 4 typical zones unique to the FSW joint, to be specific the base material, TMAZ, HAZ and NZ and in addition the transition zone for weld joints made utilizing distinctive

welding parameters is depicted in the micrographs (Fig. 5-8). All the NZ are portrayed by fine equiaxed grains with various sizes, which are produced by recrystallization in the welding process. The diverse cooling rates and weld temperature dispersion extraordinarily impacts the grain measure disparity, whereby a slower cooling rate with high temperature field will tend to frame greater recrystallized fine equiaxed grains. In any case, since no extra cooling substance was utilized, all the parameter varieties in this study created practically indistinguishable cooling rates

Henceforth, by contrasting the NZ appeared in Fig. 5-8, parameter varieties specifically 1400 rpm with 0.8 mm/s in Fig. 8 encountered the uppermost temperature field. Therefore, it is deduced that either high tool rotation speed or low traverse speed outcomes high welding temperature magnitudes in the weld nugget zone. Base materials (BM) of aluminum 6061 heat treated with T6 condition are likewise depicted in Figure. 5-8. The main strengthening particles of needle like fine precipitates is hardly visible while small coarse second phase particles were observed. The microstructure of the parent material comprises of elongated grain morphology (pancake shaped grains) having the size of 85.0 μm. Strain-hardening effects due to the rolling process during the production process caused it to have high hardness.



Figure 5:Micrographs for the locations indicated with 5X magnification (upper row) and 20X magnification (bottom row) for rotation and traverse speed of 650 rpm, 0.8 mm/s in the advancing side (AS). (low rotation speed and low traverse speed)

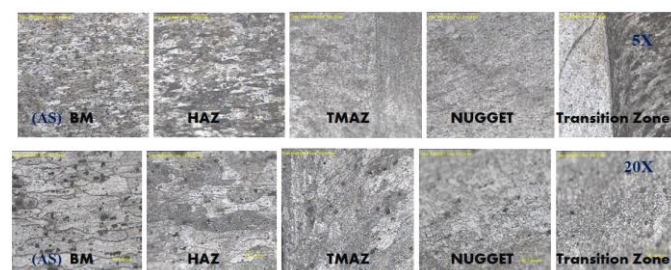


Figure 6: Micrographs for the locations indicated with 5X magnification (upper row) and 20X magnification (bottom row) for rotation and traverse speed of 650 rpm, 4.55 mm/s in the advancing and retreating sides. (low rotation speed and high traverse speed)

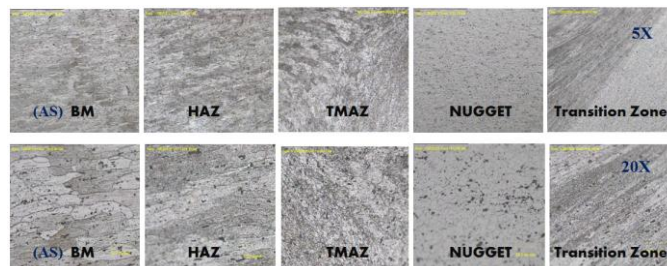


Figure 7: Micrographs for the locations indicated with 5X magnification (upper row) and 20X magnification (bottom row) for rotation and traverse speed of 950 rpm, 4.55 mm/s in the advancing and retreating sides. (moderate rotation speed with high traverse speed)

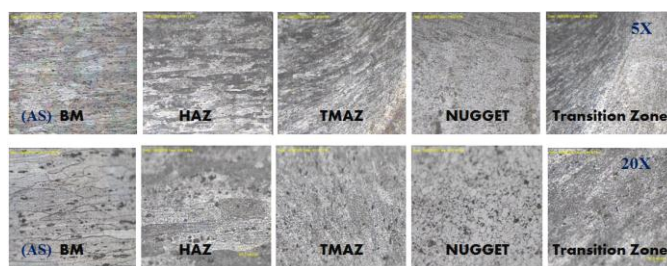


Figure 8: Enlarged micrographs for the locations indicated with 5X magnification in the upper row and 20X magnification in bottom row for rotation and traverse speed of 1400 rpm, 0.8 mm/s in the advancing and retreating sides. (high rotation speed with low traverse speed)

The second phase particles are available in an extensive amount in the HAZ in contrast to the TMAZ which shows evident material flow with the existence of smaller second phase particles. The rotation of extended grains belonging to the parent metal is largely influential of the TMAZ characterization as shown in Fig. 5-8.

Despite the fact that the grains are plastically disfigured and thermally influenced, the positioning of the grain parallel to the direction of rolling in the base material is not clearly seen. This trend is portrayed in all the parameter varieties with differed grain sizes. The NZ comprises of little second phase particles and fine equiaxed grains. Tiny holes were clearly seen in NZ as the second phase particles failed to completely dissolve as a result of inadequate heat input. The NZ is principally portrayed by small dots which are hypothetically considered as GP-1 zones. It is indicated that the premier precipitates in the 6061-T6 alloy are dissolved in the welding process and these dot-like precipitates re-precipitate homogeneously in the following cooling [124]. Insufficient heat input due to higher traverse speed values is detrimental to the formation of homogeneous grains at the NZ in contrast to lesser traverse speed values which is seen to encourage homogeneous grain development.

B. Tensile Strength

Fig. 9 and Fig. 10 shows the tensile strength distribution for FSW AA 6061 with varied governing parameters, namely the rotation and traverse speed. The values shown in these figures represent the average value taken from 3 tensile tests executed with error bars indicating a 95% confidence limit. The obtained specimens from the FSW plates were carefully examined to ensure that the specimens were defect-free.

The highest achievable tensile strength values of the friction-stir-welded AA 6061 obtained showed that the ultimate tensile strengths (UTS) and the yield strength decreased by 23 and 40 percent respectively compared to the base material tensile strength of 273MPa. All rotation speeds used observed a comparable pattern wherein an increase in the UTS was observed with increased traverse speed while keeping the rotation speed constant, except for the speed value of rpm 1400 which surprisingly depicted similar values of the tensile strength distributions although the traverse speed was increased. An acceptable joint strength efficiency of 50 to 60 percent from the parent material UTS was achieved with lesser travers speeds coupled with varied tool rotation speed values.

The lowest tensile strength values was obtained when using traverse speed of 0.8 mm/s while increased tool rotation speeds with constant traverse speed depicted a steady increase in the UTS values for all parameter combinations used. Interestingly, for the traverse speed of 4.55 mm/s, the tensile strength was seen to gradually increase with increased tool rotation speed and attain the highest magnitude of the UTS at 950rpm before abruptly experiencing a sharp drop in the UTS value when the RS was further raised to a speed of 1400 rpm. It is noteworthy that lowermost tensile strength value was attained when using the lowest rotation speed combined with the lowest traverse speed. In contrast, the highest tensile strength value was obtained when the combination of the highest value of traverse speed namely 4.55 mm/s was used medium tool rotation speed of 950 rpm. Fig. 9 and 10 is depicts the summary of these trends

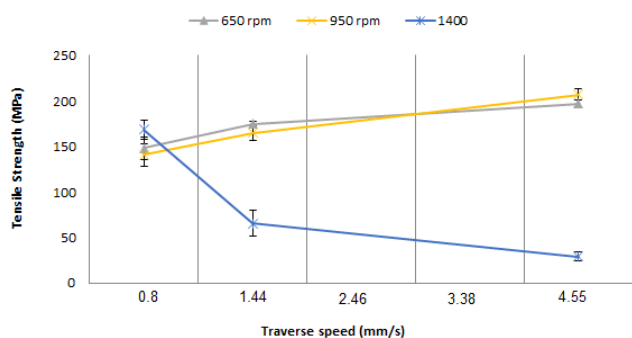


Figure 9: Tensile strength of varied FSW parameters with constant rotation speed and increased traverse speed with Error bars indicating a 95% confidence limit

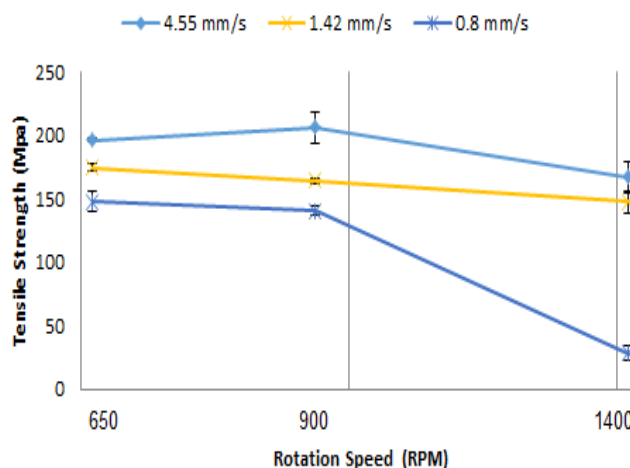


Figure 10: Tensile strength of varied FSW parameters with constant traverse speed and increased rotation speed with Error bars indicating a 95% confidence limit

Adequate heat input generated from the stirring and mixing of the material plastically is seen as the main reason behind the upsurge of the UTS values with increased traverse speeds. In addition to that, a slight increment in the material ductility is also witnessed upon gradual increment of the traverse speed. This mainly attributed to the large amount of heat developed that occurs during the utilization of higher traverse speeds, which restores the material ductility enlarging the grain size and recrystallization mechanism. The results also confirm that medium rotation speed values combined with escalated traverse speeds the obtained UTS values as well as the ductility are slightly higher as depicted in Fig 10. Earlier findings from the mentioned literatures [8] are affirmative with this analogue.

C. Sub-Surface Hardness

Measurements to obtain the hardness profile across the cross sectional area of the friction stir welded Al6061-T6 butt joint was performed in all the weld zones unique to the FSW specifically the base material, NZ, HAZ and TMAZ. Both the advancing and the retreating sides of the butt joint were measured to obtain the hardness profile for the mentioned zones. Fig 10 depicts the hardness profile crosswise the cross sectional area in the base material as well as the weld zone for a rotation speeds kept constant combined with a variation of traverse speeds.

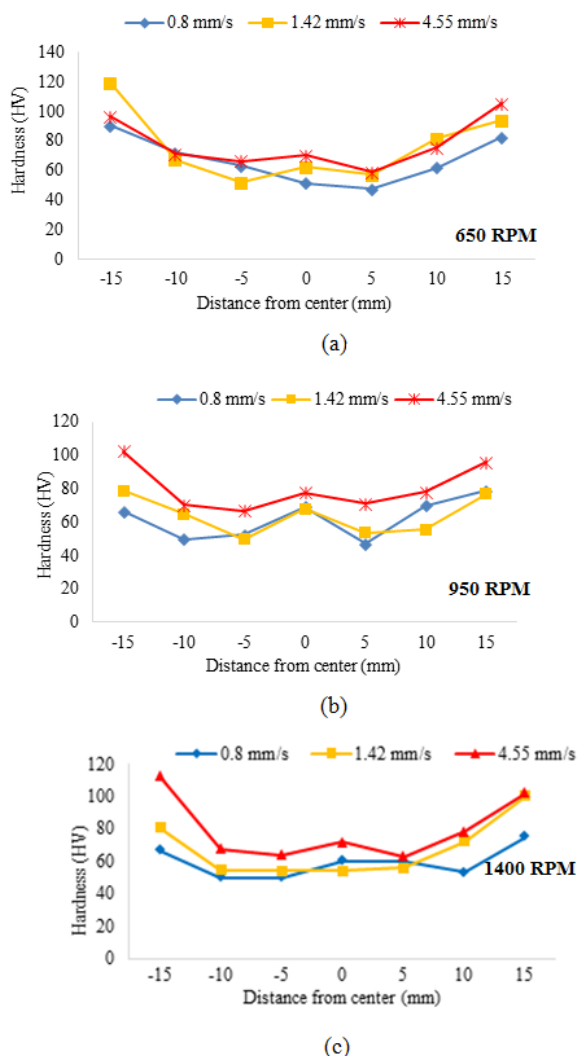


Figure 11: Friction Vickers hardness profiles in the weld zone and parent material for different variations of rotations speed (a) 650 rpm (b) 950 rpm and (c) 1400 rpm

The parent material hardness distribution was found to be between a range of 105 and 110 HV. In FSW, removal of strain hardening occurs significantly due to the dynamic recrystallization which severely softens the nugget zone compared to the parent metal. Thus, it results in a sharp drop in the hardness distribution profiles in the near the boundaries of the stir zone as well as the thermomechanically affected zone. The hardness values in both the RS and AS in the locality of the stir zone boundary was found to be varied between 50-80 HV mainly caused by the significant softening occurrence.

The obtained results showed that the AS displayed a visibly wider significantly softening region compared to the RS. Previous research has shown that several strengthening precipitates such as the GP-I zones, GP-II zones (or β''), and β -Mg₂Si is contained in AA6061 [7]. The cycle of heating and cooling which occurs during the welding process encourage the growth as well as the dissolution of the precipitates mentioned above. The high density of fine needle shaped β'' precipitate is

the main strengthening source for AA6061-T6, but it is a metastable transient phase and may be dissolved and evolve to β''' and β -Mg₂Si phase during the welding [8]. It is likely that the β'' and β -Mg₂Si precipitates in the middle part of NZ are dissolved by the heat generated in the welding process. Consequently, GP zones precipitate in the following cooling of the weld. Thus, the softening of NZ occurred [9].

The hardness measurements in both the TMAZ and NZ in the AS recorded an increment as the rotational speeds were kept constant while increasing the traverse speed. Rotation speeds of 950 rpm and 1400 rpm respectively observed pronounced increments in the above mentioned zones. A similar trend of increased hardness values was also observed in the region of TMAZ as well as the NZ when tool rotation speeds were increased while keeping the traverse speed constant. The highest hardness values were recorded at a rotation speed of 1400 rpm.

A mixture of a 'basin' and 'W' shapes was depicted in the hardness profile shape across the cross sectional area for the tool rotation speed of 1400 rpm while rotation speed 950 rpm formed usually obtained 'W' shaped profile and 650 rpm depicted a 'basin' like shape. The hardness measurements the TMAZ decreases severely compared to the parent material hardness values while a modest increment is observed in the stir zone. Both the AS and RS have similar trends. However, marginally higher hardness values were recorded in the advancing side in compared to the retreating side. The presence of fine-grain size in the stir zone is at greater traverse speed is attributes as the main reason for that.

As demonstrated in Fig. 9 and 10, the hardness measurement profile and the tensile strength in addition to the quality of FSW AA 6061-T6 may differ in a very pronounced manner with varied governing parameters. Two parameter combinations namely rotation speed 950 rpm with 4.55 mm/s traverse speed as well as 650 rpm rotation speed with 4.55 mm/s traverse speed showed excellent tensile properties combined with reasonable hardness values without any visual weld defects.

CONCLUSION

The present study was able to conclude the following:

1. Fatigue resistance and the ultimate tensile strength are shown to increase with escalated traverse speeds.
2. Increased rotation speed combined with lower traverse speeds considerably deteriorates the mechanical properties.
3. Insufficient heat input greatly influence the formation of weld defects in weld zone.
4. Higher heat input and the occurrence of homogeneous grains occurs when marginally high rotational speed is combined with high traverse speeds resulting in obtaining

the best mechanical properties for the FSW AA 6061 butt joint.

5. Two parameter variations displays a combination of good weld quality and mechanical properties namely rotation speed 950rpm with 4.6 mm/s traverse speed as well as 650 rpm rotation speed with 2.4 mm/s traverse speed

REFERENCES

- [1] D. M. Rodrigues, a. Loureiro, C. Leitaó, R. M. Leal, B. M. Chaparro, and P. Vilaça, "Influence of friction stir welding parameters on the microstructural and mechanical properties of AA 6016-T4 thin welds," *Materials & Design*, vol. 30, no. 6, pp. 1913–1921, Jun. 2009
- [2] I. Lim, S. Kim, C. Lee, and S. Kim, "Tensile Behavior of Friction-Stir-Welded Al 6061-T651," vol. 35, no. September, pp. 2829–2835, 2004
- [3] Lakshminarayanan, A.K., and V. Balasubramanian. "Tensile and Impact Toughness Properties of Gas Tungsten Arc Welded and Friction Stir Welded Interstitial Free Steel Joints." *Journal of Materials Engineering and Performance*, no. 1 (2011): 82-89
- [4] S. R. Ren, Z. Y. Ma, and L. Q. Chen, "Effect of welding parameters on tensile properties and fracture behavior of friction stir welded Al–Mg–Si alloy," *Scripta Materialia*, vol. 56, no. 1, pp. 69–72, Jan. 2007.
- [5] Arbegast, William and Hartley, Paula (1998), "Friction Stir Weld Technology Development at Lockheed Martin Michoud Space Systems – An Overview," *Proceedings of the 5th International Conference on Trends in Welding Research*, Pine Mountain, GA., June.
- [6] G. D'Urso, E. Ceretti, C. Giardini, and G. Maccarini, "The effect of process parameters and tool geometry on mechanical properties of friction stir welded aluminum butt joints," *International Journal of Material Forming*, vol. 2, no. S1, pp. 303–306, Dec. 2009.
- [7] Dongxiao L, Xinqi Y, Lei C, Fangzhou H, Hao S. Effect of welding parameters on microstructure and mechanical properties of AA6061-T6 butt welded joints by stationary shoulder friction stir welding. *Materials and Design* 64:251–260 · December 2014..
- [8] Indira Rani, Marpu R. N. and C. S. Kumar, A study of process parameters of friction stir welded AA 6061 aluminum alloy in O and T6 conditions, *ARPN Journal of Engineering and Applied Sciences*, vol. 6,
- [9] S. Rajakumar, C. Muralidharan, V. Balasubramanian, Establishing empirical relationships to predict grain size and tensile strength of friction stir welded AA 6061-T6 aluminium alloy joints, *Transaction Nonferrous Met. Soc. China* 20(2010) 1862-1872